

Harnessing the Sun's Gravity for LEO to GEO transfers

By Stijn DE SMET,¹⁾ Jeffrey S. PARKER,²⁾ and Daniel J. SCHEERES¹⁾

¹⁾University of Colorado at Boulder, Boulder, CO, USA

²⁾Advanced Space, Boulder, CO, USA

This paper introduces a new type of transfer between inclined circular low-Earth orbits and geostationary orbits. Traditionally, the required inclination changes are achieved through out-of-plane maneuvers. For this new type of transfer, by properly timing and orienting the initial orbit, all inclination change and periapee raise is performed by solar gravity. For high start inclinations, the required ΔV can be significantly reduced from the more traditional geostationary transfer options.

Key Words: Geostationary, Solar tide effects

Nomenclature

e	:	eccentricity
i	:	inclination
M	:	mass
\hat{n}	:	normal unit vector
P	:	orbital period of the Earth around the Sun
\hat{t}	:	tangent unit vector
r_p	:	periapee radius
\mathbf{x}	:	converged state
$\tilde{\mathbf{x}}$:	predicted state
ΔV	:	change in velocity
ω	:	argument of periapee
Ω	:	longitude of ascending node

1. Introduction

In 1964, Syncom 3 became the first satellite to be launched into a geostationary orbit (GEO). Ever since, the geostationary orbit has achieved widespread popularity among mission designers through its unique features. Proof of that are the more than 500 satellites currently active in GEO. GEO satellites are commonly launched from Guiana Space Centre, Kennedy Space Center and Baikonur Cosmodrome. The lowest inclinations that can be achieved for each launch site without dog-leg maneuvers are 5, 28.5 and 51.5° respectively. Hence, for high latitude launch sites, a large part of the ΔV budget needs to be allotted to the inclination changes (Δi).

The transfers of interest for this research are from inclined circular orbits at 185 km altitude to a geostationary orbit; a circular, equatorial orbit at an altitude of 35,786 km. Several strategies exist to minimize the fuel cost for such transfers. Examples are a two-burn strategy where the Δi is optimally distributed over the two burns and three-burn bi-elliptic or super-synchronous transfers where the Δi is performed at a high altitude. Both are briefly explained in the next paragraphs.

The two-burn transfer option achieves the inclination and altitude change in one transfer orbit. At a node crossing in the initial circular orbit, the first maneuver raises the apoapse to the geostationary altitude and reduces the inclination by

an amount Δi_1 . The satellite then traverses the transfer orbit to its apoapse at geostationary altitude. There, a second maneuver reduces the eccentricity and inclination to zero. The distribution of the performed inclination changes over the two maneuvers can be optimized to minimize the overall ΔV budget. Examples of such optimization procedures for different initial inclinations can be found in Figure 1.

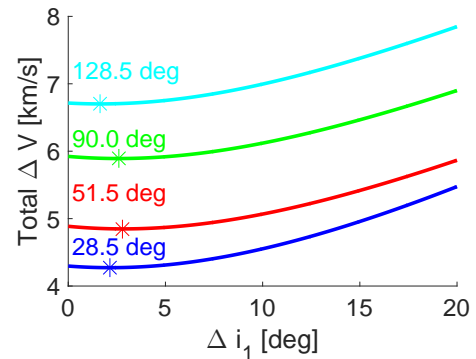


Fig. 1.: Two-burn strategy: ΔV cost as function of Δi_1 .

A three-burn bi-elliptic transfer leverages the fact that inclination changes require the least fuel when applied at low velocities, e.g., at a high apoapse. The bi-elliptic transfers are composed of two consecutive transfer orbits. At a node crossing of the initial circular orbit, the first maneuver raises the apoapse altitude above the geostationary altitude. This transfer orbit is followed up to apoapse. Here, a second maneuver is executed that raises the periapee from the initial value to the geostationary altitude. This maneuver also nearly nullifies the inclination. This second transfer orbit is followed down to periapee. There, a third maneuver is performed to circularize the orbit. In theory, the transfer requires the least ΔV when apoapse is at infinity and the inclination change can be performed for free. However, this requires infinite time of flight. In Figure 2a, one can see a few examples of the trade-off between time of flight and fuel cost for bi-elliptic transfers for different initial inclinations. In Figure 2b, the optimal two-burn strategies for different inclinations are compared to the theoretical minimum of the bi-elliptic transfers. For start inclinations larger than 38.365°, the optimal two-burn

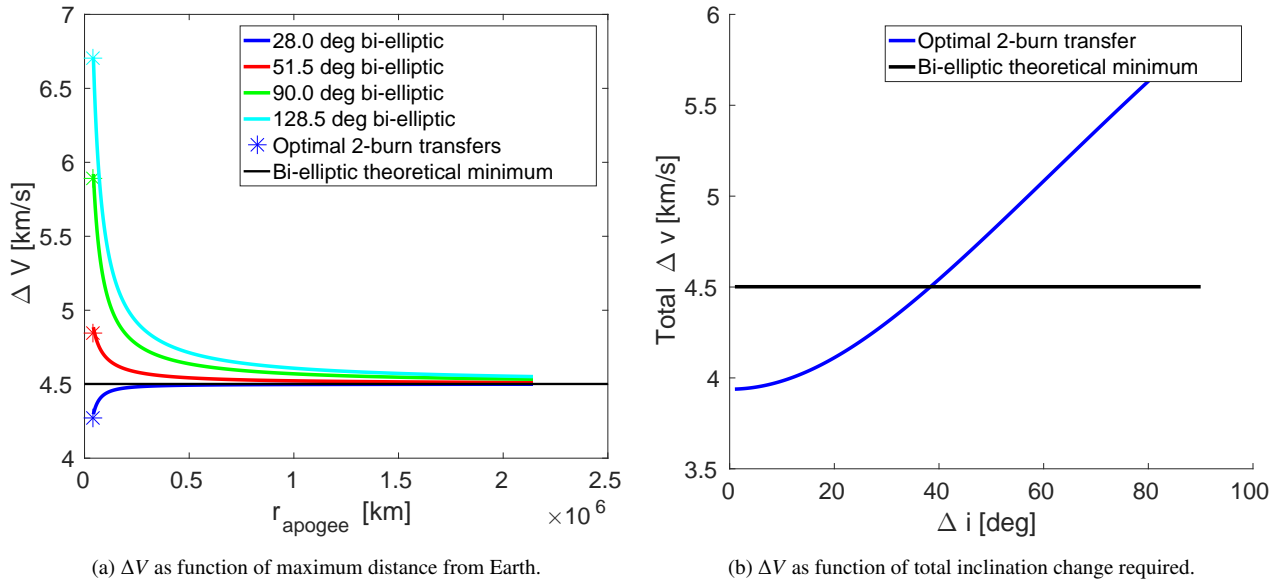


Fig. 2.: Comparisons between two- and three-burn strategies.

strategy has a higher fuel cost than the theoretical minimum for bi-elliptic transfers. Note that this value is specific for the transfers from 185 km to geostationary altitude.

Significant fuel savings can be realized using the bi-elliptic strategy on transfers with a high initial inclination. Those transfers fly far away from Earth and have a high time of flight. This presents a new opportunity; the further you get from the Earth, the stronger the perturbation of the Sun becomes. For the discussion and analysis above, this effect has been ignored. An approach has been identified in Ref. 1), wherein the Sun's gravity may be fully utilized to perform the plane change and periapee raise using minimal fuel, if any. This strategy will be further investigated in this paper.

These transfers leave LEO after an in-plane impulse in the velocity-direction. Throughout the transfer, solar gravity perturbs the orbit such that the next periapee occurs at GEO altitude with 0° inclination. Then, another in-plane impulse in the anti-velocity direction re-circularizes the orbit. This strategy and the bi-elliptic transfer are visualized in Figure 3. Both transfers depart with identical orbital elements, but the Sun-perturbed orbit does not require an out-of-plane maneuver at apoapse to execute the plane change. Ref. 1) has found transfers for an initial 51.5° inclined orbit that require only 2.5% more fuel than the classic two-burn transfers from 28.5° , the common transfers for launch from Kennedy Space Center. Therefore, this technology increases flexibility in launch site selection for GEO spacecraft.

The solar perturbations add complexity to the design of the transfers. While the two- and three-burn strategies have no dependence on the relative geometry between the Sun, the Earth and the orbit, this geometry will determine the perturbing acceleration on the orbit. Assuming fixed initial r_p and i , the design variables are time of year of LEO departure, initial transfer eccentricity (e), argument of periapees (ω) and right ascension of ascending node (Ω). Note that the time

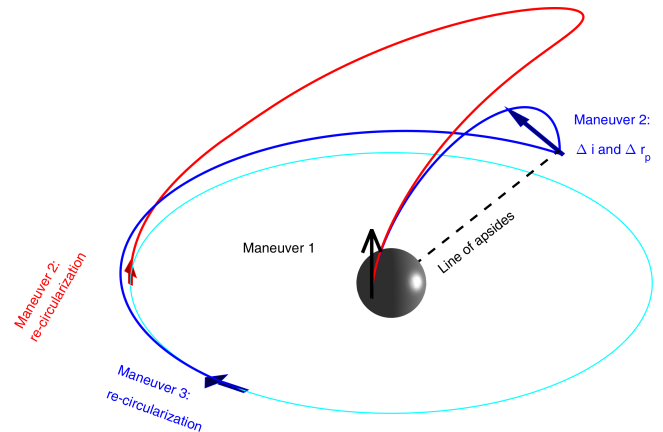


Fig. 3.: Visualization bi-elliptic (blue) and Sun-perturbed orbit (red). Not to scale.

of year is computed w.r.t. to the J_{2000} epoch. Navigating the four-dimensional state space is not trivial, especially given the sensitive maps between design variables and final r_p and i values. In this paper, the initial conditions for transfers at different times of year, with resolution one day, and for three different initial orbital inclinations are identified. This requires finding intersections between contour surfaces representing the correct Δr_p and correct Δi in (ω, Ω, e) -space, at the smallest e they occur. By minimizing e , the required fuel to inject the spacecraft from LEO into its transfer orbit is minimized.

In the next section, the used methodology will be summarized. Next, the developed methodology will be used to design transfers throughout the year for different start inclinations, e.g., different potential launch sites. Finally, the transfers will be compared to the classic two- and bi-elliptic transfers based on time of flight and fuel budget.

2. Methodology

In this chapter, the four building blocks of the developed methodology will be briefly discussed. The first building block maps a given set of initial conditions to the next periapse. This is used in the second building block: a single-shooting method to find a set of initial conditions that satisfy the required periapse raise. The third block uses this functionality within a continuation technique to compute all points with the correct periapse-raise. Local minima on this contour can be identified. The fourth building block traces the local optima out in eccentricity until the maximum inclination change for that local optima is obtained. In the next sections, each of the four blocks will be explained in more detail. Finally, it will be explained how the four building blocks co-operate in a single algorithm.

2.1. Building block 1: Poincaré map

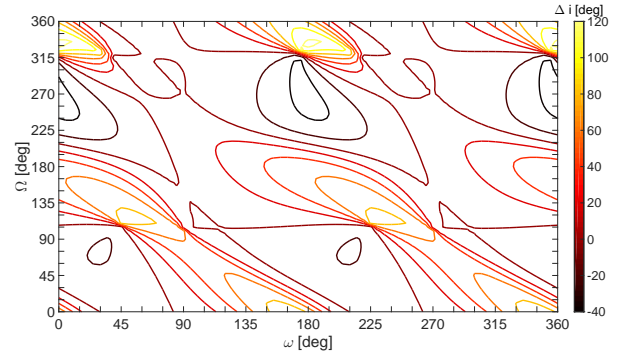
The transfers are designed to attain the periapse raise and inclination change in one orbit. Therefore, the initial state must be integrated from periapse to periapse. This has been done through a Poincaré map where the flow between two periapse surface of section crossings is numerically integrated.

To perform this integration, the Hill problem dynamical system is well suited. This model assumes that the primary body is much more massive than the secondary and that the third body is massless. Hence, the two massive bodies only experience gravitational attraction from the other massive body and orbit their center of mass. This orbit is assumed to be circular. Hence, one body revolves around the other body with constant angular velocity. These are good assumptions for this system given $M_{Sun} = 1.99e30 \text{ kg} > M_{Earth} = 5.97e24 \text{ kg} \gg M_{SC}$ and the Earth's actual eccentricity of 0.0167.³⁾ Finally, the Hill problem assumes that the spacecraft is much closer to the secondary than to the primary body. This is representative for the transfers of interest, as they will need to stay in close proximity to the Earth to have reasonable transfer times.

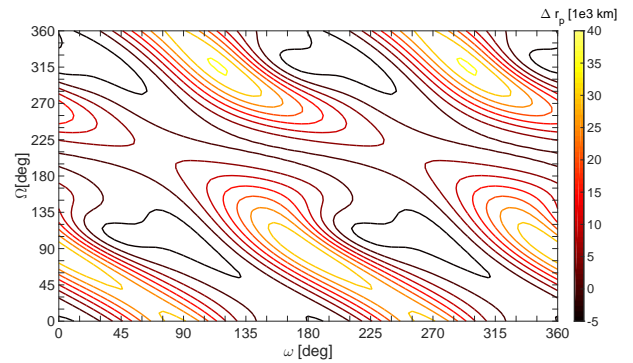
Using this map, the periapse and inclination change can be computed for different sets of initial conditions. Keeping the time of year, e , initial r_p and initial i constant, Figure 4 shows the periapse and inclination change for the entire range of possible ω and Ω values. Clearly defined contour lines for the inclination and periapse raise can be observed. This figure also showcases a useful symmetry of the Hill problem: the realized periapse and inclination change are the same for $(a, e, i, \omega, \Omega)$ and $(a, e, i, \omega + \pi, \Omega)$. Therefore, the ω design space can be halved; $\omega \in [0, \pi)$. The Hill problem also has a temporal symmetry. The periapse and inclination change for a set of initial orbital elements at time t and time $t + 0.5P$ are identical, with P the orbital period of the secondary around the primary. Therefore, the temporal design space can be halved; $t \in [0, 0.5P)$, e.g., day 0 to 182.5. Through the temporal and ω -symmetry, the design space can be reduced by a factor four.

2.2. Building block 2: Find point satisfying required periapse raise

The developed periapse-to-periapse map method can be used within a single-shoot method to find a set of initial orbital



(a) Inclination change contours.



(b) Periapse change contours.

Fig. 4.: Contours for day 0, $i_0 = 51.5^\circ$, $e_0 = 0.9856$.

elements that raise the periapse altitude by 35,601 km from the original 185 km to GEO altitude. For this method, all initial conditions are kept fixed, except for ω and Ω .

First, an initial set of orbital parameters is mapped using building block 1 to compute the final r_p . Using a forward finite difference step method, the partials of r_p with respect to ω and Ω are computed. The required change in both angles is then predicted, after which building block 1 is used to evaluate the periapse at this state. This procedure is repeated until the required periapse raise is achieved, within a 100 km tolerance.

2.3. Building block 3: Find contour satisfying required periapse raise

Building block 2 provides a set of initial conditions (ω, Ω) that realize the desired periapse raise. This point can be used to find all combinations of (ω, Ω) that realize the desired periapse raise, while keeping all other initial conditions fixed. To this end, a continuation method is developed. From Figure 4b, it is known that the periapse contours have turning points. Therefore, a pseudo-arclength continuation method⁴⁾ has been selected, which is known to be robust around turning points.⁵⁾

At the initial point \mathbf{x}_0 , the partials of r_p with respect to ω and Ω are computed using a forward finite difference step method. Using this information, the tangent unit vector $\hat{\mathbf{t}}$ can be computed. By selecting a certain step size Δs , the new predicted state is $\tilde{\mathbf{x}}_1 = \mathbf{x}_0 + \Delta s \hat{\mathbf{t}}$. Computing the periapse raise at this predicted state completes the predictor step.

The corrector step is then performed under the pseudo-arc length constraint: the dot product between the tangent direction and the difference between the previous point (\mathbf{x}_0) and the next point (\mathbf{x}_1) must equal Δs . Hence, \mathbf{x}_1 is enforced to be on the line through $\tilde{\mathbf{x}}_1$ with a direction perpendicular to $\hat{\mathbf{t}}$; $\hat{\mathbf{n}}$. The geometric interpretation of this can be seen in Figure 5.

By computing the gradient of the periaapse raise at $\tilde{\mathbf{x}}_1$ along the $\hat{\mathbf{n}}$ -direction, the next corrected state can be predicted. Here, building block 1 is used to assess the realized periaapse raise and the gradient along the $\hat{\mathbf{n}}$ -direction is computed again. This Newton method is iterated until convergence. Based on the number of required iterations, the step size Δs is adjusted and the process is repeated for the next point.

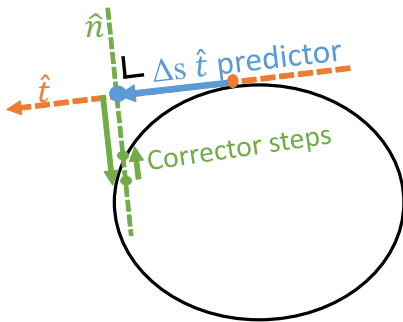


Fig. 5.: Pseudo-arc length continuation method.

This method can be used to compute the periaapse raise contours. In Figure 6, the periaapse contour plots for different values of eccentricities have been depicted. One can see that at small eccentricities, multiple periaapse contours exist, which grow in size and merge at a certain eccentricity. The number of local maxima of the inclination change (indicated by the colored dots) is not constant. Starting with one local optima per contour line, a V-shape appears where the local optima branch off. From then on, there are two local optima per contour line. When the two contours merge into one, the V-shaped pattern prevails. Hence, there are four local optima on that contour line. For all cases encountered, a maximum of four local optima has been found.

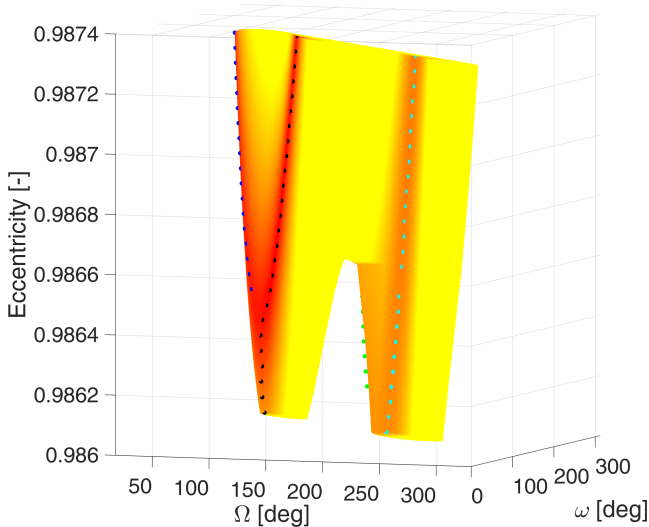


Fig. 6.: Contour plots for different eccentricities.

2.4. Building block 4: Follow inclination gradient on periaapse contours

Figure 6 demonstrates that the local maxima move smoothly. Therefore, computing complete contours for every eccentricity is unnecessary. It is more efficient to compute the local optima on a contour for one eccentricity. Then, using building block 2, at a new eccentricity, a point on the contour line is found in the neighborhood of the previous optima. A modified version of building block 3, where the continuation is performed in the direction of largest inclination reduction and stopped at a local optima, is used to find the local optima at that eccentricity. This is repeated for different eccentricities until the maximum Δi is found for that local optima family. An example of this procedure can be found in Figure 7, where the green and blue stars are respectively the local maxima on the full contour plot for the initial eccentricity and the maxima for each family in eccentricity. A limit of 0.99 has been imposed on the eccentricity. For those very eccentric orbits, the TOF between two periaapses becomes very large, and in some cases infinite, meaning they escape the Earth system. This causes numerical issues with the developed algorithm.

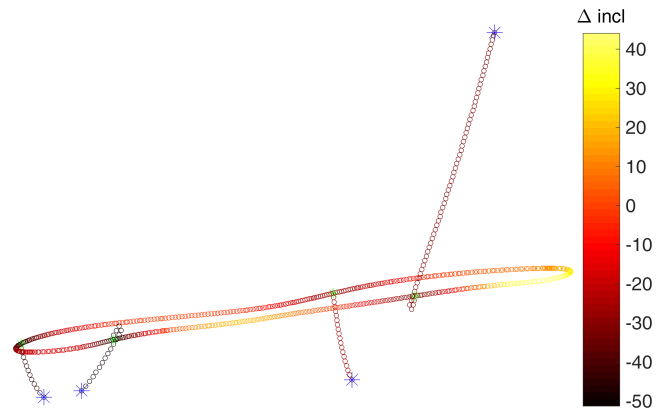


Fig. 7.: Evolution of the four local minima in eccentricity.

2.5. Full algorithm

Building block 3 is used on different eccentricities, until an eccentricity is found with a single, closed contour with four local optima. Then, for each local optima on this contour, the eccentricity that results in the minimal achievable inclination is determined using building block 4. These are the results for that day and can be used as initial guesses for the next day.

3. Results

The developed method has been applied to three different initial inclinations that capture the entire range of possible launch sites between Baikonur and polar latitudes. Furthermore, the retrograde counterpart of the Baikonur launch latitude has been investigated. The results for start inclinations 51.5° , 90° and 128.5° can be found in Figure 8 where one can see how the four local optima evolve over the year. The initial e , ω and Ω are plotted, which combined with the fixed initial i and r_p fully determine the initial state of the trajectory. The first row shows the realized i change. Only the first 182 days of the year have been computed, as the results for the next half of the year are identical through the temporal symmetry of the Hill system.

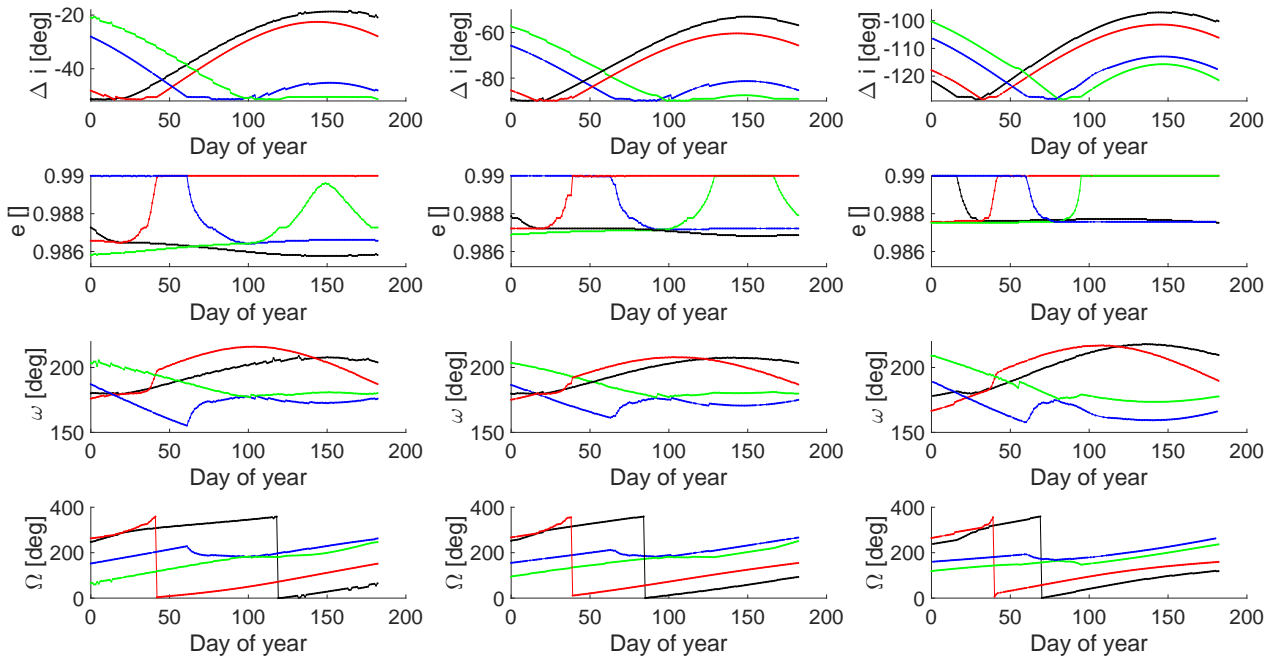


Fig. 8.: Comparing the four different families for the three different start inclinations. From left to right: 51.5°, 90° and 128.5°.

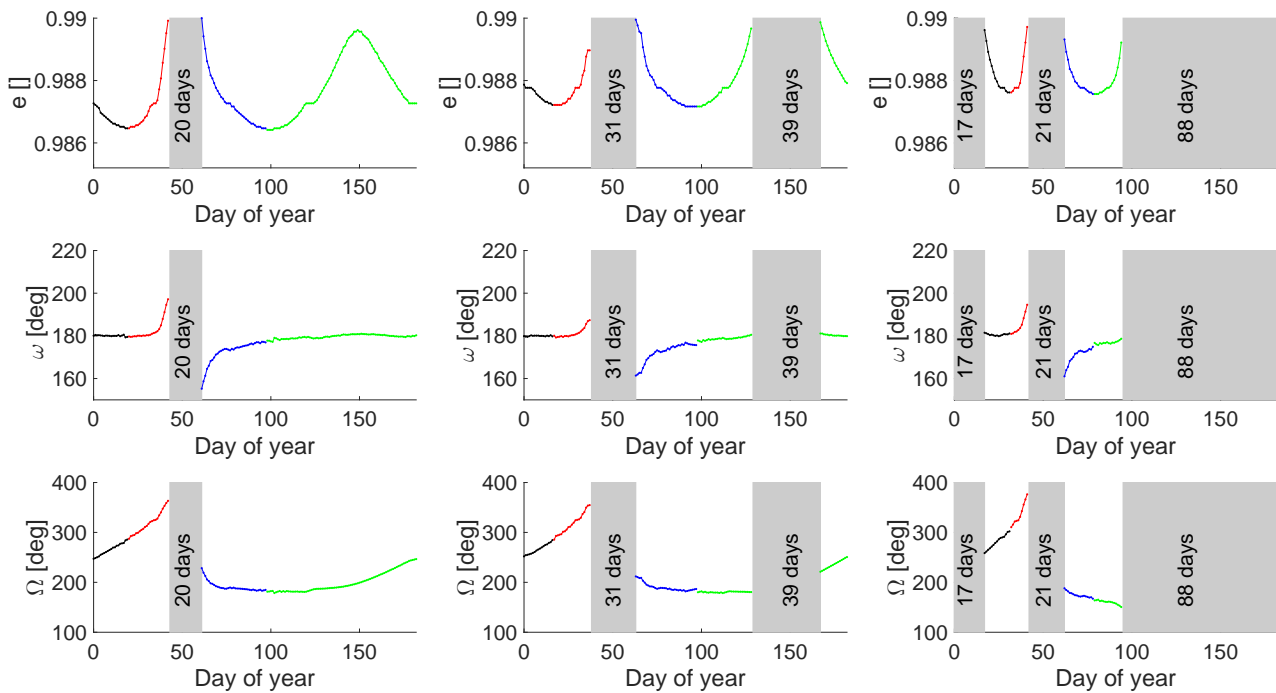


Fig. 9.: Feasible trajectories 51.5° (left), 90° (middle) and 128.5° (right).

For higher initial inclinations, it can be observed that the families start at higher eccentricities. Hence, the 0.99 eccentricity cut-off is reached earlier. Examples of this can be seen for the 128.5° case, where for the first 16 days, the 0.99 eccentricity cap is active on the black family, explaining why the inclination cannot be reduced fully. Another example is the green family curve, which reaches the 0.99 cut-off between days 129 and 166 for the 90° case. Similarly, for the 128.5 degree case, it reaches it at day 95. Hence, for higher required inclination changes, less days have a feasible transfer. Figure 9 shows the initial orbital elements for the feasible transfers, and indicates

in grey when and for how long the transfers are infeasible. A transfer is deemed feasible when the second periapee condition is within one degree inclination and 100 km periapee altitude of a geostationary orbit. For an initial i of 51.5°, 90° and 128.5°, respectively 325, 225 and 113 days per year have feasible trajectories. One can observe very similar structures for the initial elements. At first, the ω is around 180°, after which it starts increasing strongly, at the same time as the strong increase in e . During this time, the Ω is increasing linearly. Then, the e limit of 0.99 is encountered during which no transfer is possible. After this, the ω and Ω values drop significantly, and a different

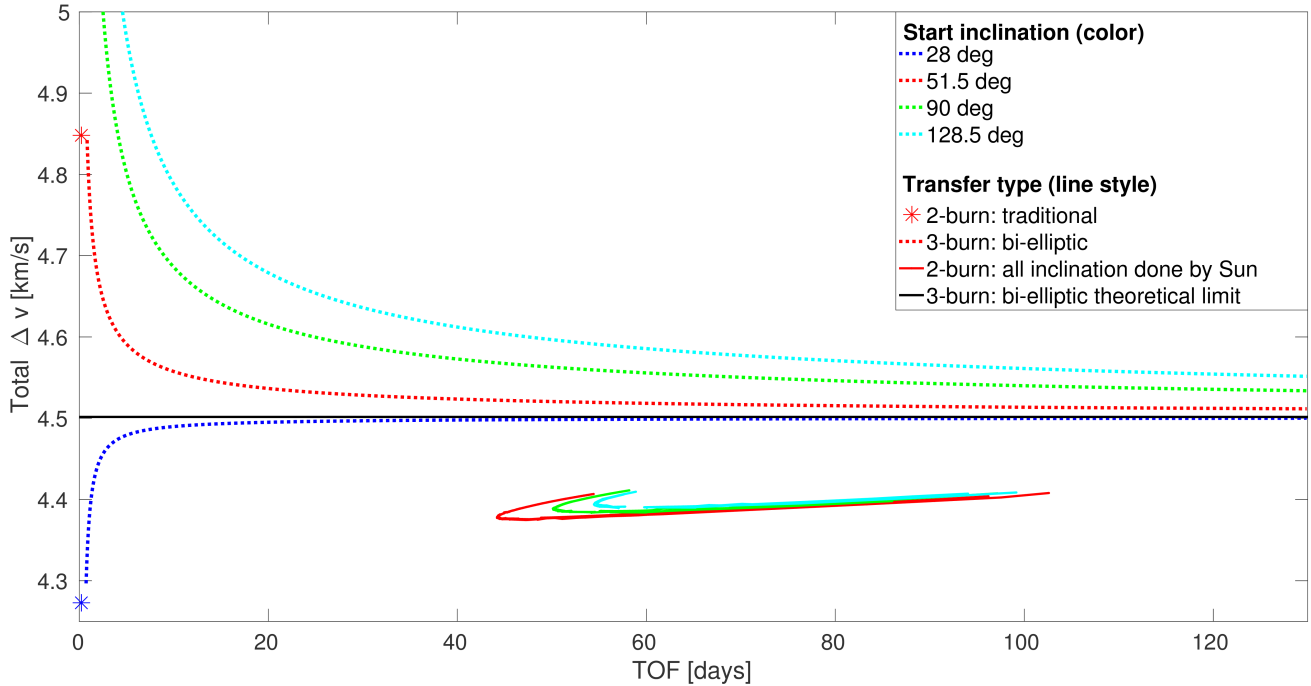


Fig. 10.: Comparison of the different transfer strategies.

family of transfers becomes feasible. The ω value increases, until it reaches 180° and stays there. To enable this, the eccentricity has to increase again. For the 90° and 128.5° scenario, the 0.99 eccentricity cut-off is reached again.

4. Conclusion and discussion

This paper identified the required initial conditions to perform a Sun-driven transfer from a low-Earth orbit at an altitude of 185 km with three different initial inclinations (51.5° , 90° and 128.5°) to a geostationary orbit. Compared to the optimal two-burn and bi-elliptic transfers, the total required ΔV for the designed transfers is smaller. Figure 10 shows the time of flight vs. ΔV for the different transfer strategies, for different values of initial inclination. The higher the initial inclination, the larger the ΔV savings are. From this figure, some disadvantages can also be identified. First, the time of flight is significantly larger than for the two-burn strategy. Second, for a specific time of year, only one trajectory, with a specific time of flight and fuel cost, has the right Sun-Earth-orbit geometry. Hence, the bi-elliptic transfers' flexibility between TOF and fuel budget is lacking. Third, not all times of year have feasible trajectories. Taking these disadvantages into account, when transfer time is considered less important than fuel savings, the new transfer

method can be a possible alternative to the classic transfers for launches from high latitudes.

Some of those disadvantages could be mitigated by relaxing the constraints on the trajectory. A significant eccentricity increase is required for a marginal reduction in the final inclination. By allowing small out of plane maneuvers during the transfer, the time of flight can be reduced and the number of feasible trajectories increased. This research can provide good initial guesses for those trajectories.

References

- 1) Geryon Space Technologies: *Multi-Body Dynamics Method of Generating Fuel Efficient Transfer Orbits for Spacecraft*, U.S. Patent 20120248253, filed March 22, 2012, and issued October 4, 2012.
- 2) Villac, B.F. and Scheeres, D.J.: The Effect of Tidal Forces on Orbit Transfers, 11th AAS/AIAA Space Flight Mechanics meeting, Santa Barbara, CA, USA, AAS 01-247, February 11-14, 2001.
- 3) de Pater, I. and Lissauer, J.J.: *Planetary Sciences*, Cambridge University Press, 2010.
- 4) Keller, H.B.: *Numerical Solution of Bifurcation and Nonlinear Eigenvalue Problems, Applications of Bifurcation theory*, editor P.H. Rabinowitz, 1977.
- 5) Chan, T.F.: Newton-Like Pseudo-Arclength Methods for Computing Simple Turning Points, *SIAM Journal on Scientific and Statistical Computing.*, **5** (1984), pp. 135–148.